Current and shot noise in double barrier resonant tunneling structures in a longitudinal magnetic field

V. Hung Nguyen and V. Lien Nguyen*
Theoretical Department, Institute of Physics, VAST, P.O. Box 429, Bo Ho, Hanoi 10000, Vietnam

T. Anh Pham
Physics Faculty, Hanoi National University of Education, 136 Xuan-Thuy, Cau-Giay, Hanoi, Vietnam
(Received 7 March 2007; revised manuscript received 30 August 2007; published 28 December 2007)

We study the resonant tunneling through double barrier structures in a longitudinal magnetic field. The study shows the necessity of taking into account both the energy dependence and the finiteness of the decay widths of the resonant energy levels, which are closely associated with interesting effects such as the hysteresis, the magnetic-field-induced negative differential conductance, and the shot noise suppression or enhancement. The Landau level quantization produces a strong fluctuation of the noise versus bias at a given magnetic field or the noise versus magnetic field at a given bias. The obtained results provide a better understanding of available experimental data.

DOI: 10.1103/PhysRevB.76.235326 PACS number(s): 73.40.Gk, 72.70.+m, 73.23.−b, 75.75.+a

The double barrier resonant tunneling structures (DBRTSs) have attracted much attention, both experimental and theoretical, since the original discovery by Tsu and Esaki.[1] Besides the very high potential device applications, these structures provide an almost ideal tool for testing different quantum properties of the electron tunneling process. The interest in DBRTSs is related to the very particular current-voltage (*I-V*) characteristics, which exhibit a strongly superlinear region at relatively low (preresonant) applied bias and a negative differential conductance (NDC) typically accompanied with the hysteresis behavior at higher bias. The hysteresis behavior, observed first by Goldman *et al.*,[2] has been attributed to the intrinsic bistability, which arises from the feedback of the electrostatic potential, induced by the electrons accumulated in the quantum well, on the tunneling current. Such an electron accumulation was also experimentally examined by Young *et al.*[3] and subsequently discussed in Refs. 4–7. Theoretically, the intrinsic bistability observed in *I-V* curves of DBRTS has been analyzed in a number of works.[8–12] Blanter and Büttiker (BB)[11] have shown that the observed hysteresis behavior is related to the interaction taken into account via the charge accumulated in the well due to capacitive coupling to reservoirs.

A magnetic field perpendicular to barriers makes the in-plane motion of electrons quantized into Landau levels, and therefore, strongly affects the coupling between the energy levels in the emitter and those in the quantum well. As a result, the *I-V* curve should have plateaulike features in the preresonant region and the width W_B of the bistable region should become field dependent. In reality, such magnetic-field related effects have been observed.[5,13] Two kinds of AlGaAs-GaAs-AlGaAs DBRTS measured in Ref. 5 correspond to different electron lifetimes in the well, much longer or about the same as the transition time. In the range of magnetic fields ≤ 6 T, while for the former DBRTS the width W_B with some fluctuation totally increases, for the latter ones it decreases rapidly and tends to zero, as the magnetic field rises. Theoretically, the magnetic-field effects on the current have been partially described in Ref. 9, where by solving self-consistently the Schrödinger and Poisson equations the magnetic-field-induced fluctuation of the width W_B as well as of the peak current was qualitatively explained as a direct consequence of the fluctuation of the density of electrons accumulated in the well.

While for the current the magnetic-field effect has been widely examined, there are only a few reports on the effect on the shot noise. It is believed that the noise should be even more sensitive than the current to the magnetic field.[14] The most interesting experimental data we have found are those reported by Kuznetsov *et al.* for GaSb-AlSb-InAs-AlSb-GaSb DBRTS.[15] The main features observed in Ref. 15 are as follows: (1) at zero magnetic field the shot noise is equal to the full shot noise value of $2eI$ in the low bias region (where e is the elementary charge and I is the current), then becomes significantly suppressed (sub-Poissonian noise), and eventually increases beyond the full shot noise (super-Poissonian noise) as the bias increases; (2) the suppression may be as strong as the noise becomes less than half of the full shot noise value; (3) a low magnetic field makes the noise oscillate with bias and the produced noise peaks may exceed the full shot noise value; and (4) the voltages at which the noise peaks occur correspond to the NDC regions in the *I-V* curve. Theoretically, the suppression and the hysteresis behavior of the shot noise at zero magnetic field have been analyzed in a number of reports.[10,11,14,16,18] Actually, the crossover from sub-Poissonian (in the positive differential conductance region) to super-Poissonian shot noise (in the bistable region) in DBRTSs has been predicted by BB.[11] Such a crossover is believed to be caused by the Coulomb interaction which affects more the shot noise than the current behavior. Moreover, assuming the decay widths associated with two barriers to be much smaller than all other energy scales in the problem, BB repredicted that the low-limiting value of the noise power spectrum S is half of the full shot noise value.[11,17] In other words, following BB the Fano factor, defined as $F=S/2eI$, should never be smaller than a half, $F\geq 1/2$. Later, Aleshkin *et al.*[18] have claimed that the BB statement of $F\geq 1/2$ is, in fact, the consequence of the assumption on the very small width of the resonant energy level. When this is not the case, calculations[18] reveal that the noise power spectrum can be considerably smaller than half the full shot noise value. Note, however, that in Ref. 18 the decay width of the resonant level was taken to be energy independent. Such a simplification may cause a loss of fine structures in the *I-V* characteristics as well as in the shot noise behavior, and particularly, does not allow us to study adequately the hysteresis behavior.[11] Actually, the effect of the magnetic field was not taken into account in both Refs. 11 and 18. The shot noise expression in a longitudinal magnetic field has been derived in Ref. 20, but, as noted by the authors, it is not evident and too complicated to be even qualitatively discussed.

The aim of this work is to calculate the current and the shot noise power spectrum in DBRTSs in the presence of a longitudinal magnetic field, taking into account both the energy dependence (neglected in Ref. 18) and the finiteness (neglected in Ref. 11) of the resonant level decay widths. The model under study essentially is an extension of that suggested by BB.[11] Besides the quantization of the motion in the longitudinal (z) direction, giving rise to the resonant energy levels E_n $(n=0,1,2,\ldots)$, the longitudinal magnetic field B causes also Landau quantization of the electron motion in the (x,y) plane. Assuming that the longitudinal and the transverse motions of electrons are separated, the total electron energy measured from the band bottom in the well is given by

$$E_{nl}=E_n+(l+1/2)\omega_c, \quad n,l=0,1,2,\ldots, \tag{1}$$

where $\omega_c=eB/m^*$ is the cyclotron frequency (the constants $\hbar$ and the light velocity are set to 1). The density of states (DOS) in the well can be factorized as

$$\mathcal{D}(E)=\mathcal{D}_\perp(E_\perp)\mathcal{D}_z(E_z), \quad E=E_\perp+E_z, \tag{2}$$

where the transverse DOS, $\mathcal{D}_\perp$, in the presence of a magnetic field has the form

$$\mathcal{D}_\perp(E_\perp)=(m^*/2\pi)\sum_l \omega_c\delta[E_\perp-(l+1/2)\omega_c], \tag{3}$$

which reduces to the standard two-dimensional DOS of $D_\perp=m^*/2\pi$, when $\omega_c\to 0$, and the longitudinal DOS, $\mathcal{D}_z$, in the Breit-Wigner limit is defined as

$$\mathcal{D}_z(E_z)=\frac{1}{2\pi}\sum_n\frac{\Gamma(E_z)}{(E_z-E_n)^2+\Gamma^2(E_z)/4}. \tag{4}$$

Here $\Gamma(E_z)=\Gamma_L(E_z)+\Gamma_R(E_z)$ is the total decay width of the single resonant level E_n and $\Gamma_{L(R)}(E_z)$ is the partial decay width for tunneling through the left (right) barrier. From the problem of transmission through a single rectangular barrier, we can write[11]

$$\Gamma_L(E_z)=\sigma_L\sqrt{E_z(E_z+\mathcal{U}-\mathcal{V})}\Theta(E_z)\Theta(E_z+\mathcal{U}-\mathcal{V}),$$

$$\Gamma_R(E_z)=\sigma_R\sqrt{E_z(E_z+\mathcal{U})}\Theta(E_z+\mathcal{U}), \tag{5}$$

where $\mathcal{V}\equiv eV$ with V being the voltage applied across the structure, $\mathcal{U}\equiv eU$ with U being the voltage drop across the right barrier, and σ_L and σ_R are dimensionless parameters. In the following for simplicity we assume that, of all longitudinal energy levels E_n, only the lowest level E_0 is relevant for tunneling, while all other energy levels are much higher.

Next, following the work of BB,[11] we derive the following expression for the current:

$$I=\frac{e}{2\pi}\int dE_\perp\mathcal{D}_\perp(E_\perp)\int dE_z\frac{\Gamma_L(E_z)\Gamma_R(E_z)}{(E_z-E_0)^2+\Gamma^2/4}\times[f_L(E_z+E_\perp)-f_R(E_z+E_\perp)]. \tag{6}$$

Moreover, for the zero-frequency shot noise power spectrum, $S_{\nu\mu}\equiv S_{\nu\mu}(0)$ $[\nu,\mu=L,R]$, we get

$$S_{LL}=(e^2/\pi)[\Lambda_L^2\mathcal{P}_1+\Lambda_L\mathcal{P}_2+\mathcal{P}_3],$$

$$S_{RR}=-S_{LR}=-S_{RL}=S_{LL}, \tag{7}$$

where

$$\mathcal{P}_1=\int dE_\perp\mathcal{D}_\perp(E_\perp)\int dE_z\frac{\Gamma_L(E_z)\Gamma_R(E_z)}{[(E_z-E_0)^2+\Gamma^2/4]^2}\times[f_L(1-f_R)+f_R(1-f_L)],$$

$$\mathcal{P}_2=\int dE_\perp\mathcal{D}_\perp(E_\perp)\int dE_z\frac{\Gamma_L(E_z)\Gamma_R(E_z)}{[(E_z-E_0)^2+\Gamma^2/4]^2}\times[\Gamma_R(E_z)-\Gamma_L(E_z)][f_L(1-f_R)+f_R(1-f_L)],$$

$$\mathcal{P}_3=\int dE_\perp\mathcal{D}_\perp(E_\perp)\int dE_z\frac{\Gamma_L(E_z)\Gamma_R(E_z)}{[(E_z-E_0)^2+\Gamma^2/4]}\times\left\{1-\frac{\Gamma_L(E_z)\Gamma_R(E_z)}{[(E_z-E_0)^2+\Gamma^2/4]}\right\}[f_L(1-f_R)+f_R(1-f_L)]. \tag{8}$$

In these expressions (6) and (8) $f_{L(R)}$ is the Fermi distribution function of the left (right) reservoir. The partial decay widths $\Gamma_L(E_z)$ and $\Gamma_R(E_z)$, following Eq. (5), depend on the voltage drop $\mathcal{U}$. For a given bias V, due to the Coulomb interaction this quantity $\mathcal{U}$ should be self-consistently determined from the total charge Q in the quantum well. Denoting the capacitance, associated with the left(right) barrier as $C_{L(R)}$, the self-consistent equations for $\mathcal{U}$ and Q are given by[11]

$$C_L(\mathcal{U}-\mathcal{V})+C_R\mathcal{U}=eQ,$$

$$Q=e\mathcal{A}\sum_{\nu=L,R}\int dE_\perp\mathcal{D}_\perp(E_\perp)\int dE_z\mathcal{D}_\nu(E_z)f_\nu(E_z+E_\perp), \tag{9}$$

where $\mathcal{A}$ is the structure area in the (x,y) plane, $\mathcal{D}_{L(R)}(E_z)$ is the partial longitudinal DOS associating with only the left (right) barrier, i.e., $\mathcal{D}_z(E_z)=\mathcal{D}_L(E_z)+\mathcal{D}_R(E_z)$, and

$$\mathcal{D}_\nu(E_z)=[\Gamma_\nu(E_z)/\Gamma(E_z)]\mathcal{D}_z(E_z), \quad \nu=L,R. \tag{10}$$

The partial decay widths $\Gamma_{L(R)}$ can be calculated by solving Eqs. (9) and (5) self-consistently.

The "interaction energy" Λ_L in the noise expression (7) is defined as $\Lambda_L = eg_L\mathcal{A}/(C_L+C_R+C_0)$ with $C_0=-e\partial\langle Q\rangle/\partial\mathcal{U}$ and $g_L=\partial\langle I_L\rangle/\partial\mathcal{U}$, where the average charge $\langle Q\rangle$ and current $\langle I_L\rangle$ are given by Eqs. (9) and (6), respectively.

The expressions (6) and (7) have been obtained for DBRTSs in a longitudinal magnetic field, taking into account the finiteness of the decay widths. Setting the field to be zero and replacing in expressions above $[(E_z-E_0)^2+\Gamma^2/4]^{-2}$ and $[(E_z-E_0)^2+\Gamma^2/4]^{-1}$ by $4\pi\Gamma^{-1}\delta(E_z-E_0)$ and $2\pi\Gamma^{-1}\delta(E_z-E_0)$, respectively (implying infinitesimal decay widths), these expressions reduce, respectively, to expressions (10) and (28) derived in Ref. 11. Without this approximation, the calculation of both the current I (6) and the shot noise power spectrum $S\equiv S_{LL}$ (7) must be performed numerically.

In order to proceed calculations we have to introduce the following parameters: the capacitances C_L and C_R associated with the left and right barriers, respectively, the decay width parameters σ_L and σ_R, the resonant energy E_0, and the magnetic field, measured by the frequency ω_c. Here, for simplicity we consider only the case of zero temperature and assume that $C_L=C_R\equiv C$ and $\sigma_L=\sigma_R\equiv\sigma$. Furthermore, we assume that the Fermi energies E_F in the two reservoirs are equal and that $E_0>E_F$. Then, choosing E_F as the unit of energy, the number of device parameters to be considered reduces to three: σ, E_0, and C. Hereafter, the capacitance, the bias, and the current density are measured in units of $m^*e^2\mathcal{A}/2\pi$, E_F/e, and $m^*eE_F^2/2\pi^2$, respectively.

For a given set of parameters σ, E_0, and C, both the I-V characteristics and the bias dependence of the shot noise power spectrum can be calculated at different magnetic fields. It is worth noting that, while in the framework of the approximation made in Ref. 11 the current and therefore the shot noise can be calculated only in a limiting range of bias, $V_a<V<V_U$, where V_a is defined as $V_a=[(C_L+C_R)/C_R](E_0-E_F)$ and V_U is the upper voltage boundary of the bistable region (V_a and V^*, respectively, in Fig. 4 in Ref. 11), in the present calculation, such a restriction is removed. The expressions (6) and (7) adequately give I and S, respectively, as continuous functions of V in a large range of bias, including the region of $V<V_a$ and the region of $V>V_U$. The calculations focus on magnetic-field effects, though even at zero field, as can be seen in Fig. 1, they may lead for the current as well as the shot noise some results, which cannot be extracted from the models used in Refs. 11 or 18

Figure 1(a) presents the I-V characteristics obtained from Eq. (6) in the case of zero magnetic field for devices with different values of the decay width parameter σ: 0.002 (dashed), 0.05 (dotted), and 0.1 (solid line) ($E_0=1.5$ and $C=1$). It should be noted that, since the current I increases almost linearly with increasing σ, the figure was made more compact by plotting I/σ rather than I along the vertical axis. It is evident from this figure that a decrease of σ leads to not only a reduction of the current, but also an essential increase of the width W_B of the bistable region. For the range of parameters analyzed, we found that $W_B\propto\sigma^{-\beta}$ with $\beta\approx 0.9$. The ideal case of infinitesimal decay widths considered in Ref. 11 corresponds just to the limit of the largest bistable region.

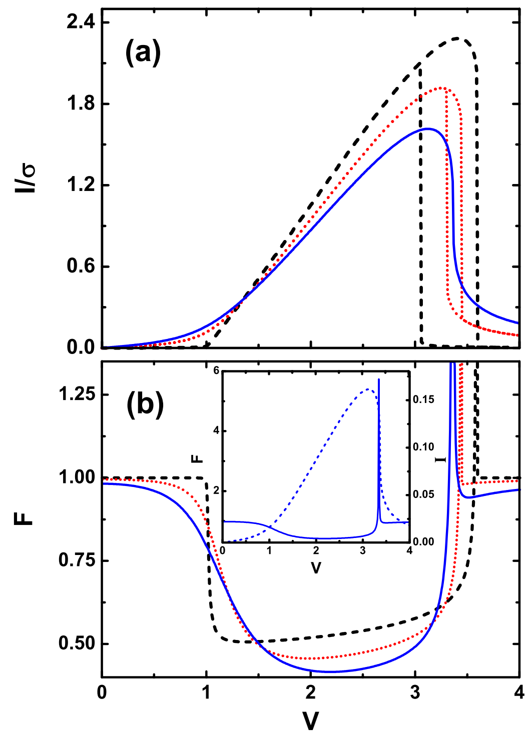

FIG. 1. (Color online) The reduced current I/σ (a) and the Fano factor F (b) are plotted against the bias V for structures with $E_0=1.5$, $C=1$, and various σ: 0.002 (dashed), 0.05 (dotted), and 0.1 (solid line), in the absence of magnetic field. In (b) the minimal values of F, $F_{\min}$, are equal to 0.42, 0.46, and 0.51 for structures with $\sigma=0.1, 0.05$, and 0.002, respectively. The enhanced noise peaks are generally too high to be fully shown in the scale. Inset in (b): $F(V)$ curve (solid line, left axis) and corresponding I-V characteristics (dotted line, right axis) are presented on the full scale for the structure of $\sigma=0.1$ (solid line in the main figure).

The role of the decay width parameter σ is even more profound on the noise behavior as can be seen in Fig. 1(b), where the Fano factor F is plotted versus bias for the same current values considered in Fig. 1(a). In general, the $F(V)$ curves obtained are similar to those reported in the literature.[15,16,18] It consists of the two limiting regions of low and high $[V>V_U]$ biases, where $F\to 1$, and an intermediate region, where the noise is first suppressed and then strongly enhanced as the bias increases. In this figure the magnitude of the suppressed as well as the enhanced shot noise is shown to essentially depend on σ. In the shot noise suppression regime, the study shows a continuous reduction of the minimal value of the suppressed noise, F_{min}, with increasing σ. For large σ values, F_{min} may become smaller than $1/2$ (see solid and dotted curves for $\sigma\geqslant 0.05$). A rough numerical estimate for the case under study ($E_0=1.5$ and $C=1$) suggests that to observe a strong noise suppression with $F_{min}<1/2$, the parameter σ must be larger than about 0.01. As was mentioned above, the shot noise suppression with $F_{min}<1/2$ has been already found in the calculation of Ref. 18. This calculation is, however, done in the simple model where the decay widths are assumed to be energy independent. Figure 1(b) not only shows the same phenomenon in our model, which takes into account the energy dependence of the decay

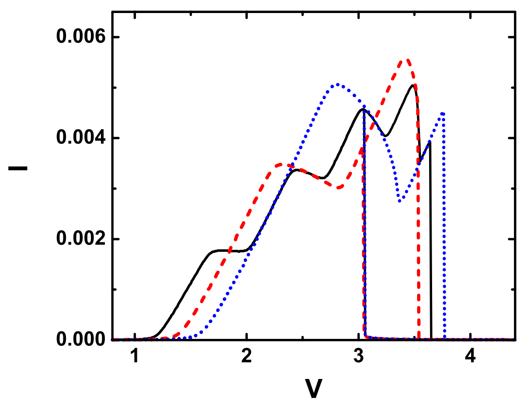

FIG. 2. (Color online) *I-V* characteristics in the presence of magnetic fields for a structure with σ=0.002, E_0=1.5, and C=1 [corresponding to the solid curve in Fig. 1(a)]. The different curves correspond to ω_c=0.2 (solid), 0.4 (dashed), and 0.6 (dotted line). Note that the lower voltage boundaries of the bistable regions in all the three curves are practically coincident in the scale.

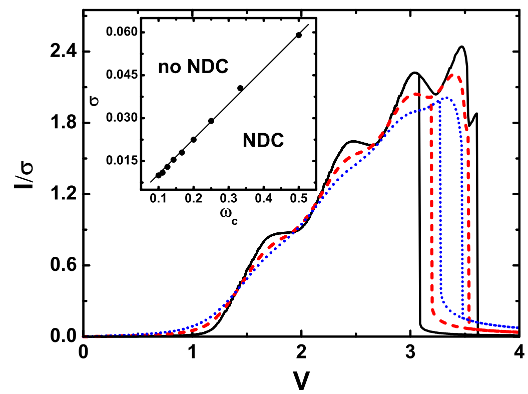

FIG. 3. (Color online) The reduced current I/σ in the presence of a magnetic field of ω_c=0.2 is plotted versus the bias V for structures with different σ: 0.005 (solid), 0.02 (dashed), and 0.04 (dotted line) (E_0=1.5 and C=1). Inset: the $(\sigma-\omega_c)$-phase diagram for observing NDC. The NDC can be observed only in the region below the straight line, which is a fit to the calculated points.

widths, but also demonstrates how F_{min} depends on the decay widths. Moreover, our study also shows an essential sensitivity of F_{min} to the energy E_0. For a given σ (σ=0.1 as an example), the value F_{min} rises almost linearly with E_0 from 0.41 for a device with E_0=1.5–0.53 for a device with E_0 =6 (measured from E_F). Since the value F_{min} is very weakly sensitive to the capacitances $C_{L(R)} \equiv C$, we suggest the following conditions for observing a strongly suppressed noise with $F_{min}<1/2$: (i) the decay widths must be not very small and (ii) the resonant level E_0 must be not very far from E_F. This explains why F cannot be smaller than 1/2 in the BB model, when the decay width is set to be infinitesimal. Thus, Fig. 1(b) confirms the possibility of the Fano factor to be below 1/2 as predicted in Refs. 18 and 19, where such a strong noise suppression was also suggested as an indication of coherent versus sequential tunneling transport.

For the noise enhancement in the NDC region, on the other hand, the smaller σ the higher the noise peak becomes. For instance, we show in the inset of Fig. 1(b) the $F(V)$ curve (solid line, left axis) and the corresponding *I-V* characteristics (dotted line, right axis) in the full scale for the case of σ=0.1 [the same solid *I-V* curve in Fig. 1(a)]. Here it is interesting to note that the Fano factor F reaches a value as high as ≈5.7, while no hysteresis has been recognized in the *I-V* curve. This agrees with experimental data reported by Song *et al.*[6] in suggesting that the charge accumulation, not system unstability, is ultimately responsible for the super-Poissonian shot noise in the NDC region. We also point out that the results presented in this inset resemble quite well Fig. 2 in Ref. 16. For devices of smaller σ, as can be seen in Fig. 1(b), the noise peaks may be too high and too sharp to be well presented.

Let us now discuss the magnetic-field effects. In Fig. 2 we present the *I-V* characteristics for the same device as that studied in Fig. 1 (dashed curves with σ=0.002), but for different magnetic fields: ω_C=0.2 (solid), 0.4 (dashed), and 0.6 (dotted line). Besides the well-known field-induced staircaselike structure in the *I-V* characteristics, this figure clearly shows that the differential conductance may even become negative in the plateaulike regions. For a given field the NDC regime becomes stronger at higher biases. On the other hand, comparing the curves corresponding to different fields, we see that the higher the field the sharper the NDC becomes. For the structure under study the magnetic field of $\omega_c \approx 0.6$ can be seen as the high limit for examining the effect of interest, when there remains only one field-induced step in the *I-V* curve. The features in Fig. 2 agree well with experimental data reported in Ref. 13 for GaAs/AlAs DBRTSs in magnetic field ranging from 2.81 to 7.18 T. It is important to note that such a magnetic-field-induced NDC could not be predicted in the approximation of Ref. 18, when the decay widths $\Gamma_{L(R)}$ are assumed to be energy independent (see inset in Fig. 5). This approximation, as is well established, could be considered acceptable only at low biases, when the NDC is still too weak to be observed.

Another important condition for realizing a magnetic-field-induced NDC is related to the decay width σ. In Fig. 3, we compare the *I-V* curves for structures with the same E_0(=1.5) and C(=1), but with different σ: 0.005 (solid), 0,02 (dashed), and 0.04 (dotted line). Here, for the same reason as in Fig. 1(a), we also plot I/σ instead of I. The magnetic field for all curves is the same, ω_c=0.2. Clearly, an increase of σ causes a smear of the steplike structure in the *I-V* curves and, consequently, a gradual disappearance of the NDC regime. A statistical analysis of numerical results for structures with E_0=1.5, C=1, and σ in the range of $0.005 \leqslant \sigma \leqslant 0.06$ and for magnetic fields in the range of $0.1 \leqslant \omega_C \leqslant 0.5$ leads to the $(\sigma-\omega_c)$-phase diagram for observing NDC shown in the inset, where the NDC can be observed only in the region below the straight line. According to this diagram, the minimal magnetic field necessary for the NDC to be observed is approximately proportional to the decay width parameter σ. Note that, even though in our calculations σ_L and σ_R are equal, since the two decay widths Γ_L and Γ_R (5) depend in different ways on not only the energy but also the bias, the structure is, in fact, asymmetric at finite biases. In the present model, when a positive voltage is set on the left reservoir, the

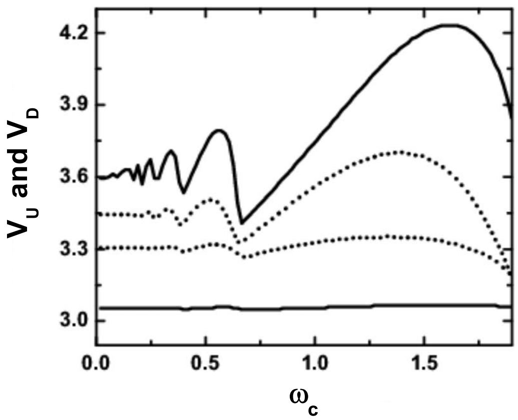

FIG. 4. Voltage boundaries (upper V_U and lower V_D) of bistable regions vary with ω_c. The two upper lines describe V_U and the two lower describe V_D. for two structures with different σ: 0.002 (solid) and 0.05 (dotted line) ($E_0=1.5$ and $C=1$).

higher the bias the smaller Γ_L and the larger Γ_R become, leading to a more asymmetric structure. Such a bias-induced asymmetry is, in fact, similar to that observed in quantum dot systems[21] and is responsible for the observed NDC. To examine this idea, the structures were made more (or less) asymmetric by reducing σ_L (or σ_R), while keeping σ_R (or σ_L) fixed. Even though not shown, the obtained results indicate an essential enhancement of the NDC when σ_L is reduced from 0.01 ($=\sigma_R$) to 0.0001, and, on the contrary, a gradual suppression of the NDC when σ_R is reduced. The NDC almost disappears for the less asymmetric structure with $\sigma_R=0.0001$ and $\sigma_L=0.01$. Orellana *et al.*[22] investigated asymmetric DBRTSs, but they did not discuss the NDC.

As for the bistable region, a nonmonotonous variation of the width W_B with an increase in the magnetic field can be already seen in Fig. 2, where it is clear that $W_B(\omega_C=0.4) < W_B(0.2)$, but $W_B(0.6) > W_B(0.4)$. A more detailed examination is shown in Fig. 4, where the lower and upper voltage boundaries, V_D and V_U, of bistable regions are plotted against the magnetic field for the two structures with different σ: $\sigma=0.002$ (solid lines) and 0.05 (dotted lines). Obviously, while the lower boundaries V_D (two lower curves) are weakly sensitive to the field, the upper ones V_U strongly fluctuate. Such a fluctuation is associated with the position of Landau levels, depending on the magnetic field, relative to the fixed position of Fermi level E_F. As the magnetic field increases, a local minimum in the $V_U(\omega_C)$ curve appears, when a Landau level is in alignment with E_F. In that case $[\omega_c(n+1/2)=E_F]$, the deepest minimum $[\omega_c\approx 0.66]$ in the $V_U(\omega_C)$ curve in Fig. 4 corresponds to the level of $n=1$. The parameters σ, E_0, and C have no direct relation to the minimum positions discussed, though they can strongly affect the magnitude of both voltage boundaries, V_D and V_U, as can be seen by comparing the solid lines for $\sigma=0.002$ and the dotted lines for $\sigma=0.05$. It is worth to mention that the results presented in Fig. 4, on one hand, are very similar to those reported in Ref. 22 and, moreover, in qualitative agreement with the experimental data reported in Ref. 5 On the other hand, they are different from the monotonous reduction of

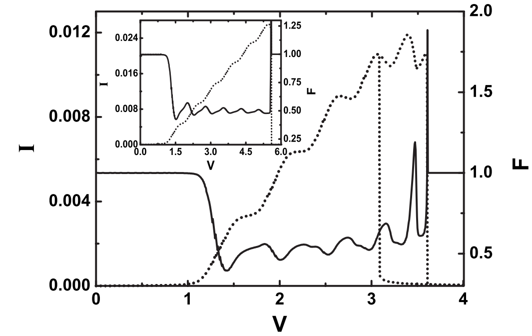

FIG. 5. Fano factor F (solid line, right axis) and the corresponding current density I (dotted line, left axis) are plotted versus V ($\sigma=0.005$, $E_0=1.5$, $C=1$, and $\omega_c=0.15$). Inset: the same as in the main figure for a structure with the same E_0, C, and ω_c, but with an energy independent decay width, $\Gamma=0.01$ [model (Ref. 18)].

bistable regions reported in Ref. 23 for the case of DBRTSs in a transverse magnetic field.

Certainly, the magnetic-field effects observed in the *I*-*V* characteristics, especially the NDC, illustrated in Figs. 2 and 3, should have an influence on the voltage dependence of the noise. In Fig. 5 we present the Fano factor F (solid line, right axis) and the corresponding current density I (dashed line, left axis) plotted against the bias V for the structure with parameters given in the figure and for a magnetic field strength, corresponding to $\omega_c=0.15$. For such a relatively weak field (see discussions later) more plateaulike regions will be produced in the *I*-*V* characteristics and therefore more interesting behaviors of the $F(V)$ dependence are expected. Actually, Fig. 5 shows a fluctuation of the factor F with typical features resembling quite well those observed in Ref. 15 In particular, the noise fluctuation is so strong that the valleys may be even lower than 0.5, while the peaks may exceed the full shot noise value. Additionally, the voltage positions of shot noise peaks are well correlated to the NDC regions in the *I*-*V* curve. Note that along with the *I*-*V* characteristics, the $F(V)$-dependence behavior strongly depends on device parameters. To obtain the $F(V)$ curves shown in Fig. 5 (for $\sigma=0.002$), which may be compared to the experimental data,[15] the typical decay width of the resonant level must be small and, certainly, the energy dependence of $\Gamma_{L(R)}$ (5) must be adequately taken into account. To illustrate the importance of taking into account this energy dependence, we plot in the inset the *I*-*V* characteristics (dashed line, left axis) and the $F(V)$ curve (solid line, right axis) for the same device and field parameters, but with the assumption of a constant (energy independent) decay width of the model.[18] Clearly, there is no NDC in the *I*-*V* curve and, accordingly, the noise fluctuation is considerably weakened.

Finally, in Fig. 6 we show the Fano factor F at a given bias, $V=2$, plotted as a function of the magnetic field measured by ω_c for three structures different only by the values of σ: 0.01 (solid), 0.02 (dotted), and 0.05 (dashed line). For each structure, the most remarkable feature observed is the fluctuation of the normalized noise F as the magnetic field increases. The higher the field, the larger the typical "period" and the fluctuation amplitude become. Such a feature in the

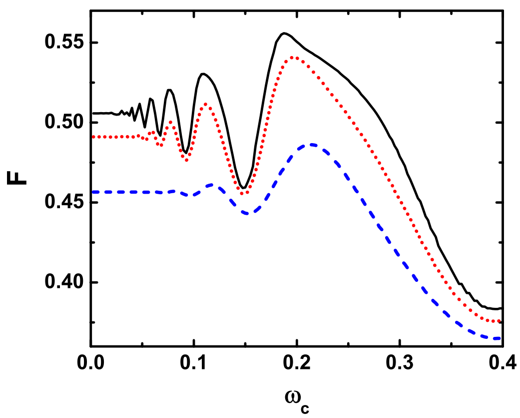

FIG. 6. (Color online) Fano factor F at a bias $V=2$ is plotted versus ω_c for three structures with different σ: 0.01 (solid), 0.02 (dotted), and 0.05 (dashed line) ($E_0=1.5$ and $C=1$).

$F(\omega_c)$ curves is a consequence of the fact that an increase in the magnetic field causes, on one hand, a fluctuation of the relative distance between the chosen bias and the center of plateaulike regions that induces a fluctuation of F. On the other hand, as the field increases, an increase of the distance between two adjacent plateaulike regions leads to an increase of both fluctuation characters, the period and the magnitude. In addition, the three curves in Fig. 6 for different σ show that from these two characters, only the fluctuation magnitude is sensitive to the decay width parameter σ: it decreases as σ increases. For the curve corresponding to the largest σ in the figure (dashed line), the fluctuation is not seen in the low magnetic-field region up to $\omega_c \approx 0.08$. This is because to see a fluctuation the magnetic field must be large enough so that ω_c is larger than the decay width of the resonant level. A fluctuation of F versus the magnetic field has been reported in Ref. 24, but for mesoscopic cavities the reported F-fluctuation behavior is different from that in Fig. 6.

We emphasize that the results reported here cannot be obtained using the models in Refs. 11 and 18 where, moreover, the effect of magnetic field was not considered. The present results qualitatively describe a number of experiments.[5,6,13,15] To make a quantitative comparison we have to determine the device parameters and the magnetic-field strength used in the experiments. While the Fermi energy E_F is entirely determined by the donor (acceptor) concentration $N_D(N_A)$ in the contacts, the energy E_0 mainly depends on the barrier height and the well width. For the AlGaAs-GaAs-AlGaAs DBRTS measured in Ref. 6 with a well of 4 nm width and a donor concentration of $N_D=1\times10^{18}$ cm^{-3}, using the barrier height of 0.31 eV and the electron effective mass of $0.067m_0$ (m_0 is the mass of a free electron), we have $E_F\approx54.3$ meV and $E_0\approx115$ meV. The experimental value $E_0/E_F\approx2.1$ is then falling well within the range of values considered in the calculations above. Furthermore, taking the resonant level decay widths to be ≈3.5 meV,[9] the typical value of the dimensionless parameter σ can be roughly estimated as ≈0.07. With the value of E_0 determined, as discussed in Fig. 1, this value of σ is too large for the hysteresis to be observed. The super-Poissonian noise in the NDC region observed in Ref. 6 has then no clear relation to the bistability. For nanodevices, in general, the super-Poissonian noise is caused by an electron accumulation and it is not necessarily accompanied by a NDC.[25]

Regarding the magnetic-field strength, for the GaSb-AlSb-InAs-AlSb-GaAs DBRTS with $N_A=2\times10^{18}$ cm^{-3} measured in Ref. 15 the value 0.15 of the dimensionless magnetic-field parameter ω_c discussed in Fig. 5 corresponds to a magnetic field of ≈7.5 T. This field is not far from those (3–5 T) used in the experiment.[15] To obtain a realistic picture of the magnetic-field-induced I-V and $F(V)$ curves, the field should be chosen appropriately: not too small so that the plateaulike regions in the I-V curve as well as a strong fluctuation in the $F(V)$ curve can be clearly seen, but not too large so that several plateaulike regions can be present. It should be mentioned that the noise is more sensitive than the current to the device parameters. For devices with $\sigma=0.05$, for example, the $F(V)$ curves (not shown) are strongly different from that in Fig. 5, independent of the values E_0 and C. Actually, for real devices there has certainly a mutual correlation between these parameters, namely, both σ and E_0 are critically related to the height of barriers.

In conclusion, we have calculated the current and the shot noise power spectrum based on a simple DBRTS model, introduced originally by BB,[11] in the presence of a longitudinal magnetic field, taking into account the finiteness of the resonant level decay widths. The study is focused on the effect associated with the magnetic field and the finite decay widths. The main results obtained are as follows: (1) the hysteresis behavior can be observed only in structures with relatively small decay widths, (2) the suppressed shot noise power spectrum in the preresonant region may be smaller than half the value of the full shot noise if the decay widths are not too small and the resonant level is not too far from the Fermi energy in the reservoirs, (3) the super-Poissonian noise observed in the NDC region is strongly correlated to the decay widths and is not necessarily accompanied by a bistable region, (4) the magnetic field may produce a NDC, which becomes stronger in structures with small decay widths and at higher biases, (5) the magnetic-field-induced fluctuation of the bistable region width is a clear manifestation of the Landau level structure, (6) the magnetic field makes the shot noise strongly fluctuate with the bias, and (7) at a given bias, the shot noise fluctuates with the magnetic field, the higher the field the larger the period and the fluctuation magnitude become. These results shed light on some controversies[17,18] about the shot noise behavior and provide a better understanding of available experimental data.

This work was supported by the Ministry of Science and Technology (Vietnam) via the Fundamental Research Program (Project No. 4.023.06).

*Author to whom correspondence should be addressed; nvlien@rop.vast.ac.vn

[1] R. Tsu and L. Esaki, Appl. Phys. Lett. **22**, 562 (1973).

[2] V. J. Goldman, D. C. Tsui, and J. E. Cunningham, Phys. Rev. Lett. **58**, 1256 (1987); Phys. Rev. B **35**, 9387 (1987).

[3] J. F. Young, B. M. Wood, G. C. Aers, R. L. S. Devine, H. C. Liu, D. Landheer, M. Buchanan, A. J. SpringThorpe, and P. Mandeville, Phys. Rev. Lett. **60**, 2085 (1988).

[4] J. F. Young, B. M. Wood, H. C. Liu, M. Buchanan, D. Landheer, A. J. SpringThorpe, and P. Mandeville, Appl. Phys. Lett. **52**, 1398 (1988).

[5] C. J. Goodings, H. Mizuta, and J. R. A. Cleaver, J. Appl. Phys. **75**, 2291 (1994).

[6] W. Song, E. E. Mendez, V. V. Kuznetsov, and B. Nielsen, Appl. Phys. Lett. **82**, 1568 (2003).

[7] Z. J. Qiu, Y. S. Gui, S. L. Guo, N. Dai, J. H. Chu, X. X. Zhang, and Y. P. Zeng, Appl. Phys. Lett. **84**, 1961 (2004).

[8] P. L. Pernas, F. Flores, and E. V. Anda, Phys. Rev. B **47**, 4779 (1993).

[9] W. Potz, Phys. Rev. B **41**, 12111 (1990).

[10] A. L. Yeyati, F. Flores, and E. V. Anda, Phys. Rev. B **47**, 10543 (1993).

[11] Ya. M. Blanter and M. Büttiker, Phys. Rev. B **59**, 10217 (1999).

[12] O. A. Tretiakov, T. Gramespacher, and K. A. Matveev, Phys. Rev. B **67**, 073303 (2003).

[13] P. J. Turley, C. R. Wallis, S. W. Teitsworth, W. Li, and P. K. Bhattacharya, Phys. Rev. B **47**, 12640 (1993).

[14] Ya. M. Blanter and M. Büttiker, Phys. Rep. **336**, 1 (2000).

[15] V. V. Kuznetsov, E. E. Mendez, J. D. Bruno, and J. T. Pham, Phys. Rev. B **58**, R10159 (1998).

[16] G. Iannaccone, G. Lombardi, M. Macucci, and B. Pellegrini, Phys. Rev. Lett. **80**, 1054 (1998).

[17] Ya. M. Blanter and M. Büttiker, Semicond. Sci. Technol. **19**, 663 (2004).

[18] V. Ya. Aleshkin, L. Reggiani, N. V. Alkeev, V. E. Lyubchenko, C. N. Ironside, J. M. L. Figueiredo, and C. R. Stanley, Phys. Rev. B **70**, 115321 (2004); Semicond. Sci. Technol. **19**, 665 (2004).

[19] V. Ya. Aleshkin, L. Reggiani, and M. Rosini, Phys. Rev. B **73**, 165320 (2006).

[20] Ø L. Bø and Y. Galperin, Phys. Rev. B **55**, 1696 (1997).

[21] H. Nakashima and K. Uozumi, Jpn. J. Appl. Phys., Part 2 **34**, L1659 (1995).

[22] P. Orellana, F. Claro, E. Anda, and S. Makler, Phys. Rev. B **53**, 12967 (1996).

[23] A. Yu. Serov and G. G. Zegrya, Appl. Phys. Lett. **87**, 123107 (2005).

[24] P. Marconcini, M. Macucci, G. Iannaccone, B. Pelle, and G. Marola, Europhys. Lett. **73**, 574 (2006).

[25] V. H. Nguyen and V. L. Nguyen, Phys. Rev. B **73**, 165327 (2006).